A fourth-order CRS moveout for reflection and diffraction events

Pedro Chira-Oliva, Martin Tygel, Peter Hubral, and Jörg Schleicher

email: *chira@ufpa.br*

keywords: *Traveltime parameterization, CRS stack*

ABSTRACT

Traveltime moveout expressions that can well stack reflection and diffraction events are of prime interest for the imaging and inversion of seismic data. In recent years, the classical hyperbolic single-parameter NMO/DMO stacking formula applied to common-midpoint (CMP) data is being replaced by new moveout expressions that make use of more parameters and allow for arbitrary measurement configurations. The advantages of the new stacking formulas are twofold. Firstly, they can fully use all the available multi-coverage data, as the source-receiver symmetry condition of the CMP configuration is no longer required. Secondly, the various parameters that are obtained by coherence analysis directly applied to the multi-coverage data are very useful for further imaging and inversion procedures. We review a fourth-order traveltime formula and examine its ability to approximate reflections and diffractions. This formula depends on the same three parameters as the hyperbolic traveltime used in the Common-Reflection-Surface (CRS) method. Synthetic examples have shown a better performance of the proposed expression compared to the second-order hyperbolic traveltime: it is more accurate within a larger aperture size.

INTRODUCTION

A significant part of seismic processing is carried out by means of stacking of multi-coverage data. The stacking is performed along traveltime moveout curves or surfaces that depend on one or more parameters. The parameters (or attributes) of the selected traveltime expression are chosen such that a coherence analysis performed on the multi-coverage data yields maximum values. As a result of the stacking process, one obtains, besides a stacked section of improved image quality, also traveltime attributes that can be used for further processing (e.g., true-amplitude attribute estimation or macro-velocity model inversion).

In the classical Common-midpoint (CMP) method, the data is organized into an ensemble of CMPs with corresponding CMP gathers. For each CMP, the corresponding CMP gather consists of source-receiver pairs symmetrically located with respect to the CMP. To stack the data along the CMP gather, one uses the normal moveout (NMO) traveltime, namely a one-parameter expression of hyperbolic type. The only attribute that is estimated in this way, is the stacking or NMO-velocity.

Over the years, methods have been designed to generalize the CMP method, so as allow the CMP gathers to include, within appropriate apertures, arbitrarily located source-receiver pairs around the CMP. In this more general situation, the CMP is called a *central point*, since it is no longer a point of symmetry within the gather. Referred in the literature as macro-model independent or data driven methods, these procedures retain the basic structure of stacking the data on appropriate gathers and along suitable traveltime moveout expressions. A survey on macro-model independent methods is provided in Hubral (1999).

To allow for an arbitrary location of source and receiver pairs, it is necessary to consider traveltime moveouts that depend on more than one parameter. In the present 2-D situation, in which multi-coverage data are recorded on a single seismic line, it is shown, under zero-order ray theory, that the traveltime for an arbitrary position of a source and a receiver around a fixed central point, depend on three parameters. The most simple and natural extension of the classical NMO traveltime is the hyperbolic moveout, which can

be readily derived as a second-order Taylor expansion of the traveltime (squared) of a primary-reflected ray around a fixed primary zero-offset reflection ray. A convenient hyperbolic traveltime expression is represented as a function of midpoint and half-offset coordinates like, e.g., the one of Ursin (1982).

The Common-Reflection-Surface (CRS) method (Müller, 1999) is one of the mentioned macro-model independent methods. Present implementations (see, e.g., Jäger et al., 2001; Trappe et al., 2001) use the hyperbolic traveltime in the form derived in Tygel et al. (1997). Thus, we call this formula the hyperbolic CRS traveltime. In this expression, the three parameters are the emergence angle, α of the normal ray with respect to the measurement surface normal at the coincident source-receiver point (called central point) and two wavefront curvatures, K_{NIP} and K_N, also measured at the central point. These curvatures refer to the normal-incident-point (NIP) wave and normal (N) wave, as introduced in Hubral (1983). A short discussion on the concept of the N and NIP waves is provided in the next section.

For the classical case of the common-midpoint (CMP) configuration, the three parameters reduce to a single (combined) parameter, namely the normal-moveout (NMO) velocity.

In the search of a more accurate traveltime, Höcht et al. (1999) have considered a reflection interface as a continuous ensemble of circular reflection elements that osculate the original reflector. The reflection response of the reflector is formulated as the superposition of the reflection responses of all the circular reflection elements that constitute the reflector.

As a result of the investigation, a new, traveltime expression, given by means of a pair of parametric equations has been has been derived. A particularly attractive feature of this representation is that it is completely described in terms of the three parameters, α, K_N, and K_{NIP} that refer to a fixed zero-offset primary reflection ray. From the system of parametric equations, a fourth-order Taylor approximation of the solution could be obtained. As expected, the corresponding second-order Taylor expansion of that solution recovers the hyperbolic CRS traveltime.

In this paper, we briefly review the derivation of the fourth-order traveltime expansion and discuss first comparisons with the more classical hyperbolic moveout. Our synthetic examples, calculated by means of ray tracing for different configurations (common midpoint and common offset), suggest that the new fourth-order expression can provide a better approximation to true traveltimes of reflection and diffraction events than the corresponding hyperbolic traveltime approximation.

THEORY

The derivation of the fourth-order CRS traveltime moveout proposed in Höcht et al. (1999) is based on the construction of the *exact* traveltime formula for the case of a circular reflector below a homogeneous overburden. As seen below, all quantities appearing in that expression can be substituted in a natural way by combinations of the CRS parameters, namely emergence angle of the normal ray, α, and the wavefront curvatures, K_{NIP} and K_N. Under this substitution, the obtained traveltime expression is expected to be a valid approximation in any media, where the CRS parameters are well defined. For practical use in an implementation of the CRS stack, Höcht et al. (1999) propose, as earlier indicated, a fourth-order Taylor expansion of the moveout that is also fully represented in terms of the three zero-offset CRS parameters.

The circular reflector

We consider the exact parametric representation of the multi-coverage reflection response of a circular reflector segment under a homogeneous overburden. The situation is depicted in Figure 1, which shows a coincident source-receiver pair at X_0. The (bold dashed) zero-offset ray from X_0 to the normal-incidence point, NIP, is the central ray with two-way traveltime t_0. The central ray emerges at X_0 under an angle α. Moreover, the (hypothetical) N and NIP waves are assumed to exhibit, at X_0, circular wavefronts with curvatures K_N and K_{NIP}, respectively.

Figure 1 also shows an arbitrary source-receiver pair (S, G) with half-offset h in the vicinity of the central point $\tilde{X}_0$. It determines the (bold) reflection ray $S\widetilde{\text{NIP}}G$ with traveltime t. Our aim is to find an approximation of the traveltime t along ray $S\widetilde{\text{NIP}}G$ in terms of the given traveltime t_0 and the CRS parameters α, K_{NIP}, and K_N of the central ray at X_0. Moreover, we wish that the moveout formula provides the *exact* expression in the case of a single circular reflector with a homogeneous overburden.

To simplify the constructions, we introduce the (bold dash-dotted) zero-offset reflection ray (see again

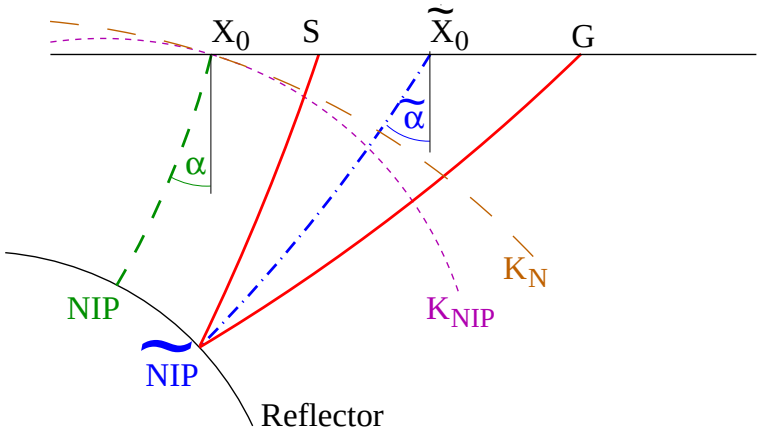

Figure 1: Reflection at a circular reflector in a homogeneous medium.

Figure 1) that is reflected at the reflection point $\widetilde{\text{NIP}}$ of ray $S\widetilde{\text{NIP}}G$. We denote its (unknown) emergence angle at the (unknown) point $\widetilde{X}_0$ by $\widetilde{\alpha}$ and its (unknown) two-way traveltime by $\widetilde{t}_0$. To find the desired expression for moveout $t - t_0$, we firstly investigate the auxiliary zero-offset moveout $\widetilde{t}_0 - t_0$ and the CMP moveout at $\widetilde{X}_0$, $t - \widetilde{t}_0$, respectively.

The image space

One of the basic ideas of the CRS approach is the introduction of a fictitious medium, called the *image space*. This is a homogeneous medium of velocity v_0, which is used to approximately compute the traveltime moveouts in the vicinity of the central point, X_0. In the image space, we construct the centers of curvature, C_N and C_{NIP}, of the N and NIP wavefronts, respectively, at X_0 (see Figure 2). We also consider the N and NIP wavefronts at $\widetilde{X}_0$ with curvatures $\widetilde{K}_N$ and $\widetilde{K}_{NIP}$ and centers of curvature C_N and $\widetilde{C}_{NIP}$. Note that the N waves at X_0 and $\widetilde{X}_0$ have the same center of curvature C_N. This is a consequence of our assumption of circular wavefronts, because this implies that the reflector in the image space (i.e., the segment that contains points C_{NIP} and $\widetilde{C}_{NIP}$) has to be circular. Its center of curvature is the same point C_N. Therefore, $\text{NIP}C_N = \widetilde{\text{NIP}}C_N$ and, thus,

$$R_N - R_{NIP} = \widetilde{R}_N - \widetilde{R}_{NIP} \ , \tag{1}$$

where $R_{NIP} = 1/K_{NIP}$ and $\widetilde{R}_{NIP} = 1/\widetilde{K}_{NIP}$ are the radii of curvature of the NIP wavefronts at X_0 and $\widetilde{X}_0$ (short dashes in Figure 2), i.e., the distances $\text{NIP}X_0$ and $\widetilde{\text{NIP}}\widetilde{X}_0$, respectively. Correspondingly, $R_N = 1/K_N$ and $\widetilde{R}_N = 1/\widetilde{K}_N$ are the radii of curvature of the N wavefronts at X_0 and $\widetilde{X}_0$ (long dashes in Figure 2), i.e., the distances $C_N X_0$ and $C_N \widetilde{X}_0$, respectively.

The traveltime difference $\widetilde{t}_0 - t_0$ in the true medium corresponds to the distance $R_N - \widetilde{R}_N$ between the wavefronts of the N waves (long dashes in Figure 2). We approximate $\widetilde{t}_0 - t_0$ by the equivalent traveltime difference $\widetilde{\tau}_0 - \tau_0$ in the image space. Here, τ_0 and $\widetilde{\tau}_0$ denote the traveltimes calculated in the image space along rays $X_0 C_{NIP} X_0$ (dashed thin line) and $\widetilde{X}_0 \widetilde{C}_{NIP} \widetilde{X}_0$ (dash-dotted thin line), respectively. Thus, we may write the desired traveltime approximation as

$$\widetilde{\tau}_0 - \tau_0 = \frac{2}{v_0}(\widetilde{R}_{NIP} - R_{NIP}) \approx \widetilde{t}_0 - t_0 \ . \tag{2}$$

Note that because of equation (1), $\widetilde{R}_N - R_N = \widetilde{R}_{NIP} - R_{NIP}$. This implies that equation (2) is exact for truly circular N and NIP wavefronts even in inhomogeneous media (see again Figure 2). Therefore, it can be expected to be a very good approximation in most seismic media.

In the same way, we approximate the (real-space) traveltime moveout, $t - \widetilde{t}_0$, by its corresponding (image space) moveout, $\tau - \widetilde{\tau}_0$, where τ_0 is defined as before and where τ is the traveltime along the ray

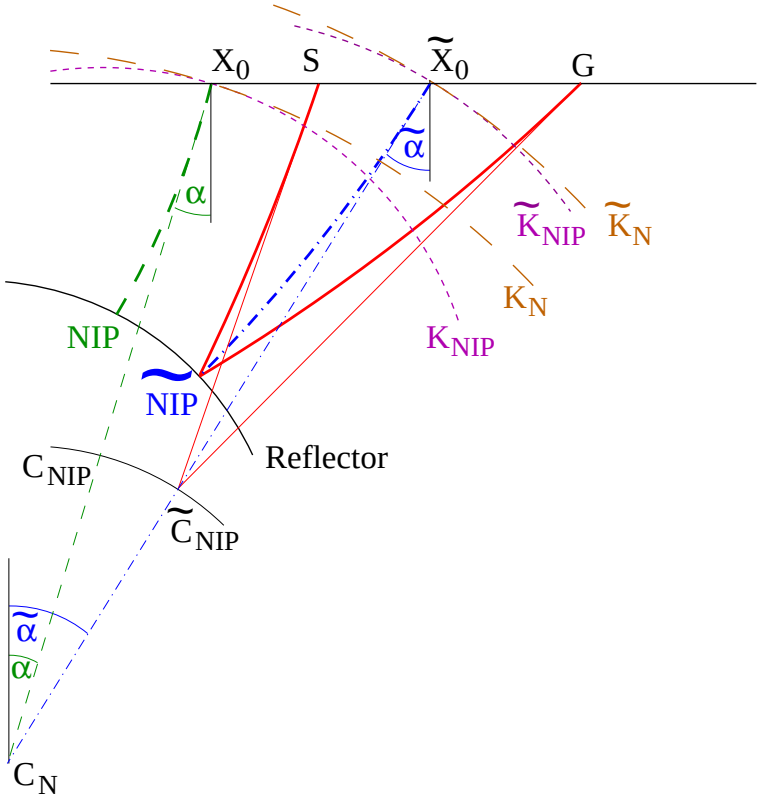

Figure 2: Centers of curvature of the N and NIP waves in the image space.

$S\widetilde{C}_{NIP}G$ in the image space. Referring again to Figure 2, we have

$$\tau - \widetilde{\tau}_0 = \tau - 2\widetilde{R}_{NIP}/v_0 \approx t - \widetilde{t}_0 \ . \tag{3}$$

The combination of the above two moveout expressions (2) and (3) yields the following relationship between the searched-for traveltime, t, and the corresponding one in the image space, τ,

$$t - (t_0 - 2R_{NIP}/v_0) \approx \tau \ . \tag{4}$$

Observe that τ is the reflection traveltime of a circular reflector in a homogeneous medium. It can be obtained from basic geometrical considerations (Höcht et al., 1999).

Traveltime for a circular reflector

As shown in Höcht et al. (1999), the traveltime τ can be expressed as a function of $\widetilde{\alpha}$, and the half-offset, h, determined by the pair (S, G), by

$$\tau^2 = \frac{4h^2}{v_0^2} + \frac{2\widetilde{R}_{NIP}^2}{v_0^2}\left(\sqrt{\frac{h^2}{\widetilde{r}_T^2}+1}-1\right) \ , \tag{5}$$

where

$$\widetilde{r}_T = \frac{\widetilde{R}_{NIP}}{2\sin\widetilde{\alpha}} \ . \tag{6}$$

In the above expressions, the unknown $\widetilde{R}_{NIP}$ geometrically relates to the given R_N and R_{NIP} (see Figure 2) as

$$\widetilde{R}_{NIP} = \widetilde{R}_N - R_N + R_{NIP} = R_N(\cos\alpha/\cos\widetilde{\alpha} - 1) + R_{NIP} \ . \tag{7}$$

Thus, squaring equation (4) and substituting τ^2 by expression (5), we obtain

$$\left[t - \left(t_0 - \frac{2}{v_0} R_{NIP}\right)\right]^2 = \frac{4h^2}{v_0^2} + \frac{2\widetilde{R}_{NIP}^2}{v_0^2}\left(\sqrt{\frac{h^2}{\widetilde{r}_T^2} + 1} - 1\right) . \tag{8}$$

This result is an approximation for the traveltime t as a function of $\widetilde{\alpha}$ and h, i.e., $t(\widetilde{\alpha}, h)$.

The last unknown in the above traveltime approximation is the emergence angle $\widetilde{\alpha}$ of the zero-offset ray at $\widetilde{X}_0$. For its determination, it needs to be related to the midpoint coordinate, x_m, of the source-receiver pair (S, G). Denoting the coordinates of X_0 and $\widetilde{X}_0$ by x_0 and $\widetilde{x}_0$, respectively, Höcht et al. (1999) find

$$x_m = \widetilde{x}_0 + \widetilde{r}_T\left(\sqrt{\frac{h^2}{\widetilde{r}_T^2} + 1} - 1\right) , \qquad \text{where} \quad \widetilde{x}_0 = x_0 \, \frac{\tan\alpha}{\tan\widetilde{\alpha}} . \tag{9}$$

Thus, the searched-for traveltime $t = t(x_m, h)$ along ray $S\widetilde{\text{NIP}}G$ can be approximated by the above pair of equations $t = t(\widetilde{\alpha}, h)$ and $x_m = x_m(\widetilde{\alpha}, h)$ parametrized by $\widetilde{\alpha}$.

The most important property of the traveltime approximation given by the parameterized equations (8) and (9) is that it is completely described with the help of the zero-offset CRS parameters α, K_{NIP}, and K_N at the central point X_0. This means it can be calculated once these parameters are given or, inversely, these parameters can be determined by fitting such traveltime curves to the seismic data. It is the latter use that we are looking for in the CRS method.

We stress once more that the parameterized traveltime given by equations (8) and (9) is based on the assumptions of circular wavefronts and a circular reflector. Therfore, it is, in principle, like the parabolic and hyperbolic traveltimes, a second-order approximation. The expectation that it will be a more accurate approximation than the latter ones is justified by the fact that underlying assumptions are more realistic, i.e., more probable to be met in practice. Thus, in the same way as practice has shown that the hyperbolic traveltime generally approximates true traveltimes better than the parabolic one, the new parameterized traveltime is expected to provide even better approximations. The first numerical tests presented in the last section of this paper confirm this expectation.

Taylor expansions

The above parametric form of the traveltime $t(x_m, h)$ cannot be conveniently used in an implementation of the CRS method. For practical use, it is thus advantageous to rewrite it as an explicit power series around $x_m = x_0$ and $h = 0$. Up to second order, i.e., in hyperbolic approximation, the corresponding Taylor expansion reads

$$t_2^2(x_m, h) = \left[t_0 + \frac{2\sin\alpha}{v_0}\,\overline{x}_m\right]^2 + \frac{2t_0\cos^2\alpha}{v_0}\left[K_N\,\overline{x}_m^2 + K_{NIP}\,h^2\right] , \tag{10}$$

where $\overline{x}_m = (x_m - x_0)$. This is the expression that has been previously derived by Tygel et al. (1997).

The fourth-order expansion has the form

$$t_4^2(x_m, h) = t_2^2 + \frac{\cos^2\alpha}{v_0^2}\left[A\overline{x}_m h^2 + B\overline{x}_m^3 + C\overline{x}_m^4 + D\overline{x}_m^2 h^2 + Eh^4\right] , \tag{11}$$

with the coefficients

$$\begin{aligned}
A &= 2K_{NIP}\sin\alpha[2 - 2v_0t_0K_N - v_0t_0K_{NIP}],\\
B &= 2K_N\sin\alpha[2 - v_0t_0K_N],\\
C &= K_N^2[5\cos^2\alpha - 4][1 - v_0t_0K_N/2],\\
D &= K_{NIP}\{2v_0t_0[3 - 4\cos^2\alpha]K_N^2\\
&\quad -[K_N(4 - 5\cos^2\alpha) + 2K_{NIP}\sin^2\alpha][2 - v_0t_0K_{NIP}]\},\\
E &= K_{NIP}^2[2v_0t_0K_N\sin^2\alpha - v_0t_0K_{NIP}\cos^2\alpha/2 + \cos^2\alpha] .
\end{aligned} \tag{12}$$

Coefficients A to E can be calculated for any given triplet of parameters α, K_{NIP}, and K_N. Therefore, expression (11) can be as easily used in an implementation of the CRS stack as equation (10).

Important configurations

For particular configurations, the above traveltime expressions reduce to simpler forms.
Common midpoint (CMP) configuration.—For the CMP configuration, we have $x_m = x_0$ or $\overline{x}_m = 0$. As a consequence, we find for the CMP traveltime

$$t^2_{4,CMP}(h) = t_0^2 + \frac{2t_0 \cos^2\alpha}{v_0} K_{NIP}\, h^2 + \frac{\cos^2\alpha}{v_0^2}\, E\, h^4 \;, \tag{13}$$

with E given above. Note that the second-order approximation, commonly known as the NMO moveout formula, depends on a single (combined) parameter,

$$v^2_{NMO} = \frac{2v_0}{t_0 K_{NIP} \cos^2\alpha} \;. \tag{14}$$

The fourth-order CMP traveltime, on the other hand, depends on two coefficients that are combinations of all three CRS parameters.
Zero-Offset configuration.—The zero-offset (ZO) configuration is characterized by the condition $h = 0$. The CRS traveltime expression reads then

$$t^2_{4,ZO}(x_m) = \left[t_0 + \frac{2\sin\alpha}{v_0}\overline{x}_m\right]^2 + \frac{2t_0\cos^2\alpha}{v_0} K_N \overline{x}^2_m + \frac{\cos^2\alpha}{v_0^2}(B\overline{x}^3_m + C\overline{x}^4_m). \tag{15}$$

Note that the second, third, or fourth-order zero-offset traveltime depend on two, three, or four coefficients that are combinations of only two CRS parameters (α and K_N).

Diffraction events

The N- and NIP-wave are fictitious waves that start at the reflection point NIP and propagate along the normal ray to the central point X_0. The NIP-wave starts from a point source at NIP while the N-wave starts from the exploding reflector at NIP.

Let us now consider the case of a pure diffraction, that is, the situation where the reflector reduces to a single diffraction point. Then, the N- and NIP-waves reduce to identical waves, both starting from a point source at NIP. As a consequence, they have identical curvatures at X_0, i.e., $K_N = K_{NIP}$. Therefore, we can use the latter identity as a *diffraction condition* in the above second- or fourth-order traveltime expressions. Upon the substitution of this diffraction condition $K_N = K_{NIP} = K$, the second-order (hyperbolic) diffraction traveltime reads

$$t^2_{2,dif}(x_m, h) = \left[t_0 + \frac{2\sin\alpha}{v_0}\,\overline{x}_m\right]^2 + \frac{4\mu\cos^2\alpha}{v_0^2}\left[\overline{x}^2_m + h^2\right] \;, \tag{16}$$

where we have introduced the notation

$$\mu = \frac{v_0 t_0}{2}\, K \;. \tag{17}$$

Note that in a homogeneous medium with wave velocity v_0, this factor reduces to $\mu = 1$.

The fourth-order diffraction traveltime is again given by equation (11) with t_2^2 replaced by $t^2_{2,dif}$. The coefficients A to E reduce to

$$\begin{array}{rcl} A &=& 4K\sin\alpha[1-3\mu], \\ B &=& 4K\sin\alpha[1-\mu], \\ C &=& K^2[5\cos^2\alpha - 4][1-\mu], \\ D &=& 2K^2[(7\cos^2\alpha - 6) - 3\mu(5\cos^2\alpha - 4)], \\ E &=& K^2[\cos^2\alpha - \mu(5\cos^2\alpha - 4)] \;. \end{array} \tag{18}$$

The application of the CRS method to seismic data using any of the so-obtained diffraction traveltime formulas will coherently stack the energy that belongs to diffraction events, thus resulting in a stacked section of diffractions rather than reflections.

It is interesting to observe the values of the above coefficients in a homogeneous medium, where $\mu = 1$, as mentioned above. We immediately see that in this situation, the coefficients read

$$\begin{aligned} A &= -8K\sin\alpha, \\ B &= 0, \\ C &= 0, \\ D &= -4K^2(4\cos^2\alpha - 3), \\ E &= 4K^2\sin^2\alpha\ . \end{aligned} \tag{19}$$

These expressions can be readily verified from a fourth-order Taylor expansion of the square of the exact diffraction traveltime of a diffractor in a homogeneous medium, which using the above variables, reads

$$t_{dif} = \frac{1}{v_0}\left(\sqrt{(\overline{x}_m - h + R\sin\alpha)^2 + (R\cos\alpha)^2} + \sqrt{(\overline{x}_m + h + R\sin\alpha)^2 + (R\cos\alpha)^2}\right)\ . \tag{20}$$

Here, $R = 1/K = v_0 t_0/2$ is the distance from the diffractor to the central point X_0.

Maximum aperture

The hyperbolic CRS moveout approximates the kinematic reflection response of a curved interface in a paraxial vicinity of the central ray. To use it in a CRS stack, it is necessary to define an appropriate aperture inside of which the approximation is sufficiently accurate. Ideally, the aperture for the CRS stack is an elliptical surface in the offset-midpoint domain. One axis is defined in the CMP section and the other in the zero-offset section (Mann et al., 2000).

The above fourth-order approximation can be used to define a practically feasible CRS aperture. Its border is located where the difference between the second- and fourth-order traveltime approximations reaches the tolerance Δt^2 for the accuracy of the traveltime approximation. In the full data volume, this is the solution of the equation

$$\Delta t^2 = \frac{\cos^2\alpha}{v_0^2}\left[A\overline{x}_m h^2 + B\overline{x}_m^3 + C\overline{x}_m^4 + D\overline{x}_m^2 h^2 + Eh^4\right]\ , \tag{21}$$

where the coefficients A to E are given by equations (12). However, the solution of equation (21) is rather complicated. Instead, the half-axes of the aperture ellipse can be approximated in the CMP and zero-offset sections.

In the CMP section, the situation is much simpler since the right-hand side of equation (21) reduces to its last term. Solving for h, we find for the aperture half-axis

$$h^{ap} = \left[\frac{v_0^2\Delta t^2}{E\cos^2\alpha}\right]^{1/4}\ , \tag{22}$$

where E is given by the last of equations (12). The same formula can be used to compute an aperture for the stack along the diffraction traveltime in the CMP section, if E given by the last of equations (18) is used.

In the zero-offset section, the terms of $\overline{x}_m^3$ and $\overline{x}_m^4$ remain in equation (21). Thus, the determination of the aperture would still require the solution of a fourth-order equation. However, since usually $K_N \ll 1$, which implies $C \ll B$, the aperture half-axis can be determined using the third-order approximation as

$$\overline{x}_m^{ap} = \left[\frac{v_0^2\Delta t^2}{B\cos^2\alpha}\right]^{1/3}\ , \tag{23}$$

where B is given by the second of equations (12). Again, the same formula can be used to compute an aperture for the stack along the diffraction traveltime in the zero-offset section, if B given by the second of equations (18) is used.

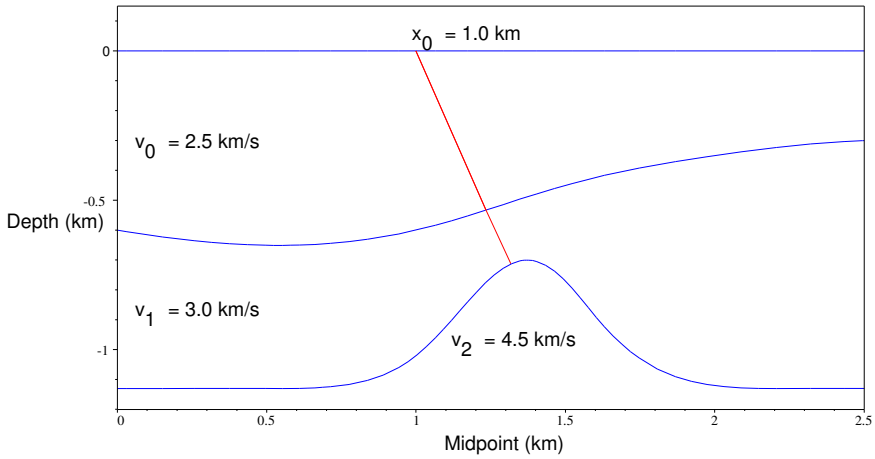

Figure 3: 2-D Earth model.

SYNTHETIC EXPERIMENTS

To demonstrate the quality of the second and fourth-order traveltime approximations discussed above, we present some simple numerical examples. They are based on the 2-D synthetic model consisting of three homogeneous layers bounded by curved interfaces depicted in Figure 3. We have compared the capability of the hyperbolic and fourth-order traveltime expansions to approximate reflections and diffraction traveltimes under different measurement configurations in the vicinity of several points X_0 at the earth's surface. One of the chosen central points X_0, together wit the corresponding zero-offset ray to the dome-like reflector, is also indicated in Figure 3. Both approximations are compared with the exact traveltimes as computed by ray tracing.

Figure 4 illustrates the traveltime approximations for the CMP configuration at three different central points. In Figure 4a, we see the exact common-midpoint reflection traveltime in the vicinity of point $X_0 = 1.0$ km (solid line) as computed by ray tracing, together with its second-order (plus signs) and fourth-order (circles) approximations. Figure 4b compares the corresponding diffraction traveltime with its approximations. As we can clearly see, the fourth-order approximation follows the true reflection traveltime curve more closely over the whole range of offsets than the second-order approximation. More or less the same behaviour can be observed in parts (e) and (f) of Figure 4, which depict common-midpoint reflection and difraction traveltimes in the vicinity of $X_0 = 1.8$ km. At the central point $X_0 = 1.4$ km (parts (c) and (d) of Figure 4), the traveltime approximations exhibit a slightly different behaviour. At this central point, both the second and fourth order traveltimes provide good approximations up to large offsets. Differently from the results of our numerical experiments at all other central points, the second order approximation is here slightly superior to the fourth order approximation.

Corresponding experiments have been realized for common-offset reflection and diffraction traveltimes for different central points and offsets. As in the case of CMP traveltimes (see again Figure 4), the diffraction traveltimes exhibit practically the same behaviour as the reflection traveltimes. We therefore restrict the following discussion to the latter.

We have calculated reflection traveltimes for four different values of the half-offset h, these being $h = 0.0$ km, $h = 0.2$ km, $h = 0.5$ km, and $h = 1.0$ km. The results in the vicinity of the same three central points $X_0 = 1.0$ km, $X_0 = 1.4$ km, and $X_0 = 1.8$ km, are depicted in Figures 5, 6, and 7, respectively. We see from parts (a) of these figures that in the chosen range of midpoints, the zero-offset traveltimes are equally well approximated by the second and fourth order formulas. At larger offsets, the fourth order formula generally provides the better approximation. An exception is again observed at the central point at $x_0 = 1.4$ km. At this point, the second-order approximation is, for a certain range of midpoints, slightly superior to the fourth-order one (see Figure 6c). Parts (d) of of Figures 5 to 7 demonstrate that neither the second nor the fourth order formula provides an acceptable traveltime approximation for offsets of $h = 1.0$ km or larger.

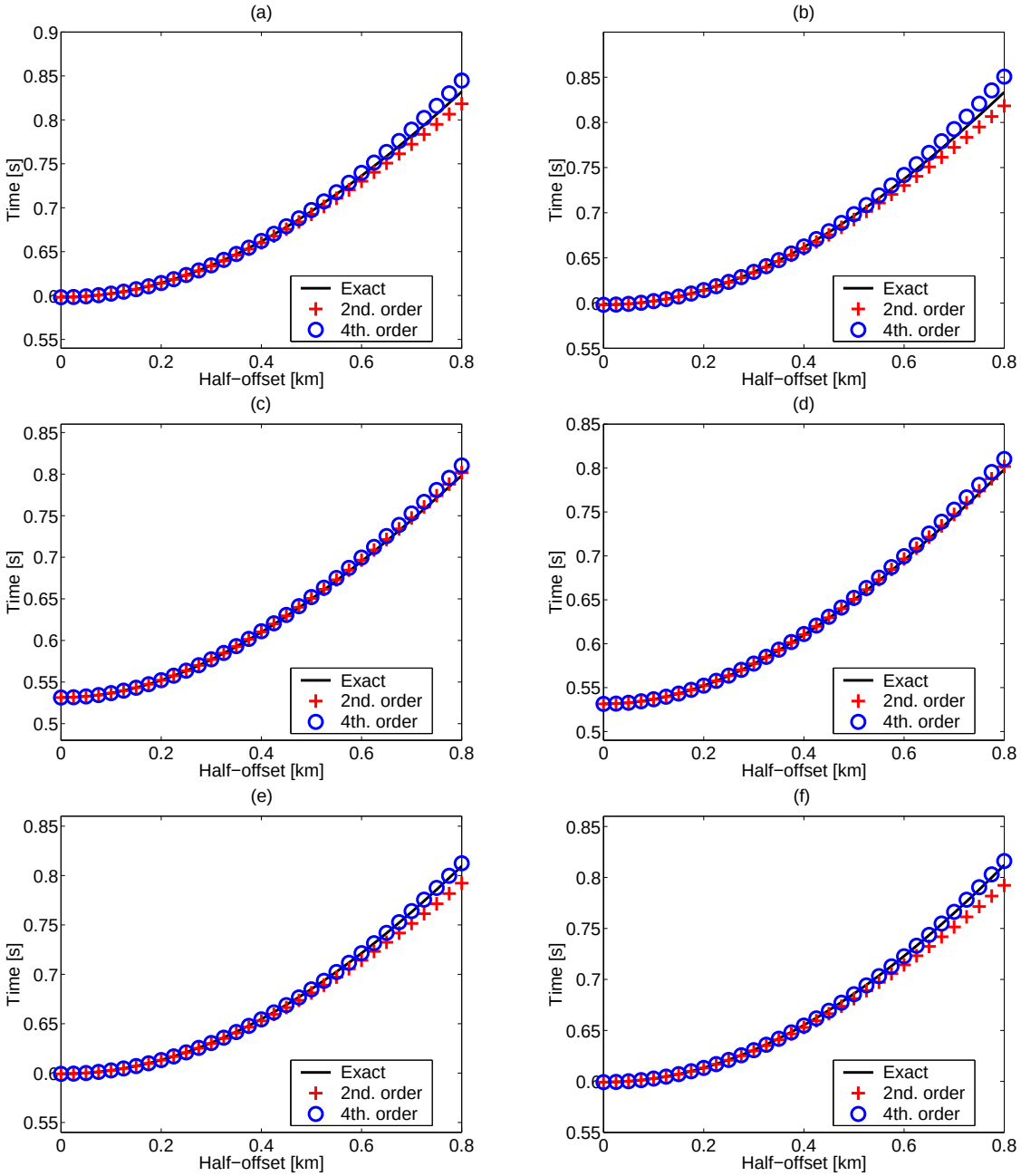

Figure 4: CMP traveltime approximations. Exact (solid line) versus second-order (plus signs) and fourth-order (circles) approximations. (a) Reflection traveltimes at $X_o = 1.0km$. (b) Diffraction traveltimes at $X_o = 1.0km$. (c) Reflection traveltimes at $X_o = 1.4km$. (d) Diffraction traveltimes at $X_o = 1.4km$. (e) Reflection traveltimes at $X_o = 1.8km$. (f) Diffraction traveltimes at $X_o = 1.8km$.

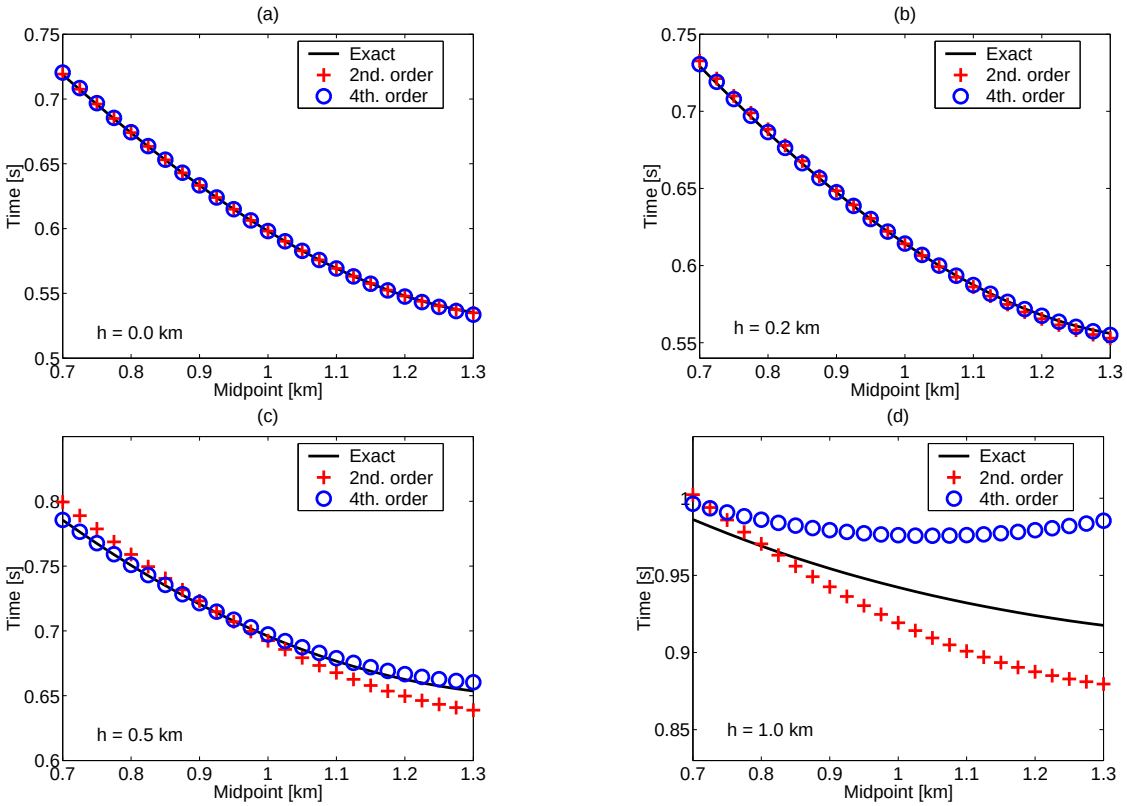

Figure 5: CO times for $X_0 = 1.0$ km. (a) $h = 0.0$ km. (b) $h = 0.2$ km. (c) $h = 0.5$ km. (d) $h = 1.0$ km.

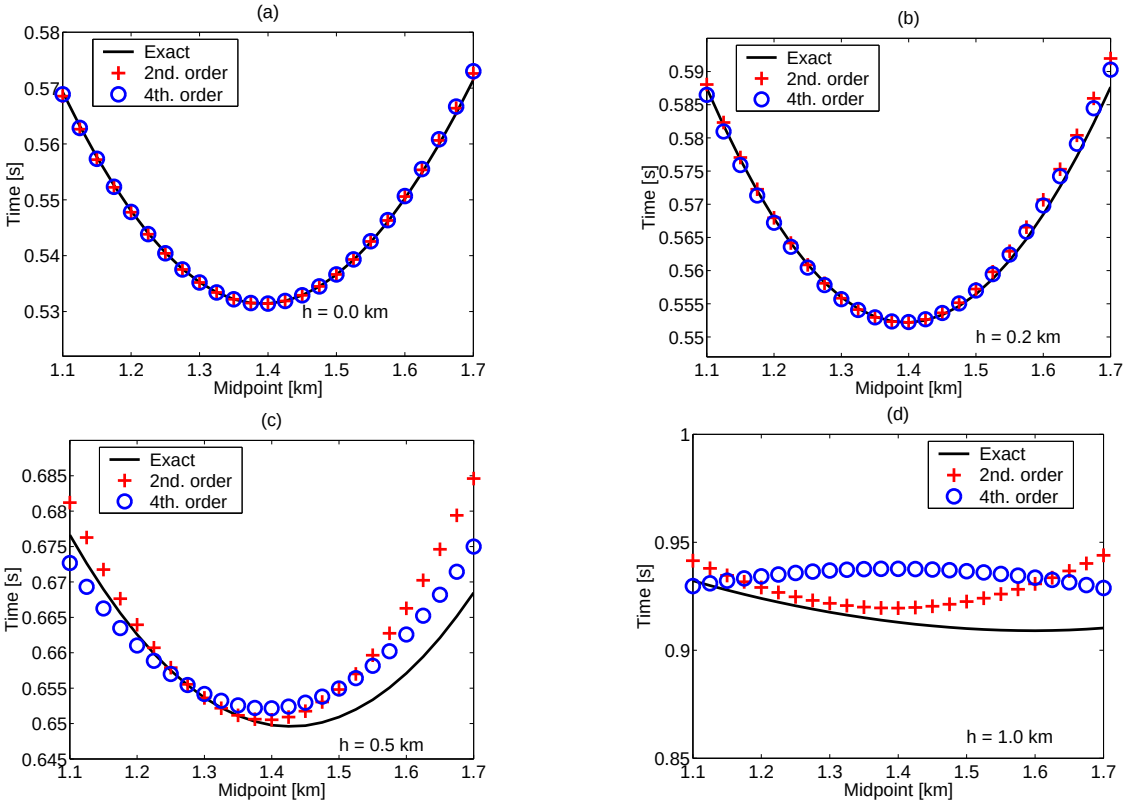

Figure 6: CO times for $X_0 = 1.4$ km. (a) $h = 0.0$ km. (b) $h = 0.2$ km. (c) $h = 0.5$ km. (d) $h = 1.0$ km.

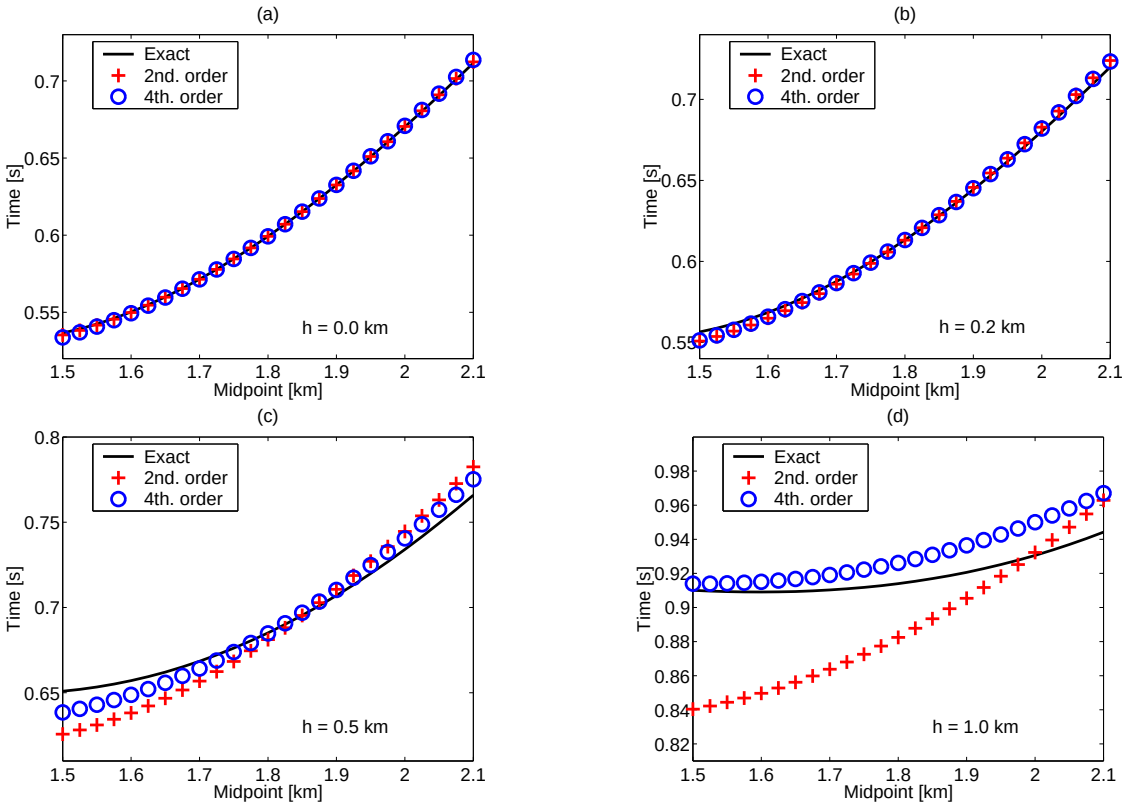

Figure 7: CO times for $X_0 = 1.8$ km. (a) $h = 0.0$ km. (b) $h = 0.2$ km. (c) $h = 0.5$ km. (d) $h = 1.0$ km.

As a general remark, we observe that our numerical experiments show a significant improvement, both in accuracy and in aperture range, of the fourth-order over the hyperbolic traveltime approximation for all configurations. The behaviour observed in the examples shown in this paper has been typical for reflections and diffractions in most of our numerical experiments. Thus, weighing in all our numerical results, we can conclude that the fourth order formula (11) generally provides more reliable approximations to the exact traveltimes than the hyperbolic traveltime (10).

CONCLUSIONS

The fourth-order traveltime moveout expression of Höcht et al. (1999) has been reviewed, implemented, and tested on a simple synthetic model. For multi-coverage data acquired along a single seismic line, this formula approximates reflection and diffraction traveltimes at coincident source-receiver pairs arbitrarily located around a reference source-receiver pair at a fixed central point. The investigated moveout expression is useful to provide simulated zero-offset sections. An attractive feature of this formula is that its coefficients depend on the same three parameters as its more conventional hyperbolic CRS traveltime counterpart. Our first results indicate that the fourth-order formula provides better traveltime approximations within a significantly larger aperture than the hyperbolic formula.

Although these result are only preliminary, we feel they are very promising for the following reasons. A CRS stack based on a better traveltime approximation, such as the fourth-order expression seems to provide, promises better stacking properties as it allows to use more data and thus more redundancy. As a result, one can expect not only better stacked sections with a higher signal-to-noise ration, but also better estimates of the CRS parameters α, K_{NIP}, and K_N. Since these parameters are the input to a velocity model building in an analogous way as the NMO or stacking velocities in the standard CMP method, their improvement should reflect in the achievable quality of the obtained velocity model.

As a second potential application for the higher-order traveltime approximation, we have seen that it can be used to define the aperture range for a CRS stack with the hyperbolic traveltime approximation. In

this way, the otherwise arbitrarily chosen aperture of the CRS stack can be replaced by one that is based on the actual traveltimes under investigation.

ACKNOWLEDGEMENTS

This work was kindly supported by the sponsors of the *Wave Inversion Technology (WIT) Consortium*, Karlsruhe, Germany.

REFERENCES

Höcht, G., de Bazelaire, E., Majer, P., and Hubral, P. (1999). Seismics and optics: hyperbolae and curvatures. *J. Appl. Geoph.*, 42(3/4):261–281. Special issue on "Macromodel independent reflection imaging".

Hubral, P. (1983). Computing true amplitude reflections in a laterally inhomogeneous earth. *Geophysics*, 48(8):1051–1062.

Hubral, P., editor (1999). *Macro-Model-Independent Seismic Reflection Imaging*, volume 105 of *Journal of Applied Geophysics*. Elsevier, Amsterdam.

Jäger, R., Mann, J., Höcht, G., and Hubral, P. (2001). Common- reflection-surface stack: Image and attributes. *Geophysics*, 66:97–109.

Mann, J., Hubral, P., Traub, B., Gerst, A., and Meyer, H. (2000). Macro-model independent approximate prestack time migration. In *Expanded Abstracts*, page B52, Glasgow. Ann. Internat. Mtg., Europ. Assoc. Geosc. Eng.

Müller, T. (1999). *The Common Reflection Surface Stack Method*. Der Andere Verlag, Bad Iburg.

Trappe, H., Gierse, G., and Pruessmann, J. (2001). Case studies show potential of common reflection surface stack - structural resolution in the time domain beyond the conventional nmo/dmo stack. *First Break*, 19(11):625–633.

Tygel, M., Müller, T., Hubral, P., and Schleicher, J. (1997). Eigenwave based multiparameter traveltime expansions. In *Expanded Abstracts*, pages 1770–1773, Dallas. Ann. Internat. Mtg., Soc. Expl. Geophys.

Ursin, B. (1982). Quadratic wavefront and traveltime approximations in inhomogeneous layered media with curved interfaces. *Geophysics*, 47(7):1012–1021.